Mon. Not. R. Astron. Soc. **346,** 905–914 (2003)

A unified treatment of the gamma-ray burst 021211 and its afterglow

Pawan Kumar★ and Alin Panaitescu

Astronomy Department, University of Texas, Austin, TX 78731, USA

Accepted 2003 August 21. Received 2003 August 15; in original form 2003 June 20

ABSTRACT

The gamma-ray burst (GRB) 021211 had a simple light curve, containing only one peak and the expected Poisson fluctuations. Such a burst may be attributed to an external shock, offering the best chance for a unified understanding of the gamma-ray burst and afterglow emissions. We analyse the properties of the prompt (burst) and delayed (afterglow) emissions of GRB 021211 within the fireball model. Consistency between the optical emission during the first 11 min (which, presumably, comes from the reverse shock heating of the ejecta) and the later afterglow emission (arising from the forward shock) requires that, at the onset of deceleration ($\sim$2 s), the energy density in the magnetic field in the ejecta, expressed as a fraction of the equipartition value (ε_B), is larger than in the forward shock at 11 min by a factor of approximately 10^3. We find that synchrotron radiation from the forward shock can account for the gamma-ray emission of GRB 021211; to explain the observed GRB peak flux requires that, at 2 s, ε_B in the forward shock is larger by a factor 100 than at 11 min. These results suggest that the magnetic field in the reverse shock and early forward shock is a frozen-in field originating in the explosion and that most of the energy in the explosion was initially stored in the magnetic field. We can rule out the possibility that the ejecta from the burst for GRB 021211 contained more than 10 electron–positron pairs per proton.

Key words: radiation mechanisms: non-thermal – shock waves – methods: analytical – gamma-rays: bursts – gamma-rays: theory.

1 INTRODUCTION

Considerable progress has been made over the last few years toward an understanding of the nature of the enigmatic gamma-ray bursts (GRBs). Much of this progress has resulted from the observation and analysis of afterglow emission – the radiation we receive after the high-energy gamma-ray photons ceases – which is firmly established to be synchrotron radiation from a relativistic, external shock (e.g. Wijers, Rees & Mészáros 1997). The nature of the explosion and the process that generates gamma-ray photons continue to be debated, although it is widely accepted that these explosions involve a stellar mass object, and γ-rays are produced in internal shocks. The detection of narrow emission lines (e.g. Greiner et al. 2003) and the emergence of a spectrum similar to that of the supernova SN 1998bw (Matheson et al. 2003) in the afterglow of GRB 030329 indicate that at least some GRBs are produced when a massive star undergoes collapse at the end of its nuclear burning life.

Further progress toward understanding the GRB explosion requires afterglow observations at times closer to the burst and a simultaneous modelling of both the afterglow and gamma-ray emissions. In this way, one can explore distance scales of $\sim 10^{16}$ cm from the centre of explosion, i.e. an order of magnitude smaller than that probed by afterglow emissions at half a day or later. Such a treatment is more likely to succeed in those cases where the prompt (burst) emission arises from the same region as the delayed (afterglow) emission, i.e. from an external shock. The simple fast-rise, exponential-decay (FRED-like) light curves seen in approximately 10 per cent of bursts represents the type expected from an external shock (Mészáros & Rees 1993), while short variability time-scale bursts with complicated light curves are usually attributed to internal shocks in an unsteady outflow (Rees & Mészáros 1994, see Piran 1999 for a review).

This paper is an attempt to explain with the same process – synchrotron and inverse Compton emission from an external shock – the burst and afterglow emission of GRB 021211 detected by the HETE II (Crew et al. 2003), a burst that had a simple, FRED-like morphology and where the afterglow has been followed starting from 60 s until 10 d after the burst. Such a simple, single-peaked light curve does not require internal shocks, which were invoked to explain multipeaked, highly fluctuating GRBs.

In Section 2 we summarize the observations of GRB/afterglow 021211. In Sections 3–6 we present the formalism for calculating the synchrotron and inverse Compton emissions from both the forward and reverse shocks (RSs), and in Sections 7 and 8 we assess the ability of the synchrotron-self-Compton model with a uniform and

★E-mail: pk@astro.as.utexas.edu

an r^{-2} stratified external medium to accommodate the properties of GRB 021211 and its afterglow.

2 SUMMARY OF OBSERVATIONS FOR GRB 021211

At a redshift of $z = 1.0$, GRB 021211 had a duration of $\sim$2.3 s in the 30–400 keV energy band and a fluence of $\sim 2 \times 10^{-6}$ erg (Crew et al. 2003); the duration in the 10–25 keV band was $\sim$4 s. If both the burst and the afterglow for GRB 021211 arise from some combination of reverse and forward external shocks, then the deceleration time t_d is close to the time when the GRB light-curve peaks in 30–400 keV band, i.e. approximately 2 s. The average flux during the first 2.3 s was 4 mJy in the 7–30 keV band, 3 mJy in the 50–100 keV band, and 0.5 mJy at 100–300 keV, while the peak of the νF_ν spectrum was at 47^{+9}_{-7} keV. The low-energy slope of the GRB flux spectrum is 0.24 ± 0.12 (i.e. $F_\nu \propto \nu^{0.24}$), while above the peak of νF_ν the high-energy spectral slope is $-1.22^{+0.14}_{-0.23}$ (Crew et al. 2003). The isotropic equivalent of the energy released in the 10–400 keV emission is $\sim 10^{52}$ erg.

At 90 s after the burst, the R-band magnitude of the afterglow was 14.06 (Wozniak et al. 2002), corresponding to a flux of 7.2 mJy. The optical flux decayed as $t^{-1.82\pm0.02}$ for the first 10 min, after which it flattened to a $t^{-0.82\pm0.11}$ fall-off (Li et al. 2003), reaching a magnitude of 25 at 7 d (Fruchter et al. 2002). The steeper decay seen during the first 10 min suggests that the optical emission is dominated by the reverse shock energizing the GRB ejecta, while the shallower, later time decay is attributed to the forward shock (FS) that sweeps-up the ambient medium. The R-band flux at 10.8 min, when the two contributions are equal, is 0.39 mJy, therefore the forward shock optical flux at 10.8 min is 0.19 mJy.

Fox et al. (2003) report a 3σ upper limit of 110 μJy on the radio (8.5-GHz) flux at 0.1 d and an upper limit of 35 μJy during 9–25 d.

Finally, Milagro has reported an upper limit of 4×10^{-6} erg cm^{-2} on the 0.2–20 TeV fluence over the burst duration reported by the HETE WXM (McEnery et al. 2002).

3 SHOCK DYNAMICS AND DECELERATION TIME

Consider an explosion where the isotropic equivalent of energy release is $\mathcal{E}$ and the initial Lorentz factor (LF) of cold baryonic material carrying this energy is Γ_0. Before the ejecta are significantly decelerated, the thermal LF $\gamma_{p,f}$ of the protons in the forward shock is equal to the bulk LF (Γ_d) of the swept-up medium, which is given by (e.g. Piran 1999)

$$\gamma_{p,f} = \Gamma_d \approx (\Gamma_0/2)^{1/2}(n_{ej}/n)^{1/4}, \tag{1}$$

where n_{ej} is the comoving particle density of the ejecta and $n = (A/m_p)r^{-s}$ is particle density in the external medium ($s = 0$ for a homogeneous medium, $s = 2$ for a pre-ejected wind). The above result holds for $n_{ej}/n \lesssim \Gamma_0^2$, otherwise $\gamma_{p,f} \approx \Gamma_0$.

Taking into account that the laboratory frame energy per FS-heated proton is $\Gamma_d\gamma_{p,f} = \gamma_{p,f}^2$, the deceleration radius R_d at which the energy of the swept-up medium is half the initial energy of the ejecta is

$$\frac{4\pi}{3-s} R_d^{3-s} A c^2 \Gamma_0 \left(\frac{n_{ej}}{n}\right)^{1/2} = \mathcal{E}. \tag{2}$$

As long as the distribution of LF of the ejecta is not too narrow, and the duration of the central explosion is less than $R/(c\Gamma_0^2)$, the comoving width of the material ejected in the explosion is proportional to R/Γ_0. Let us parametrize the comoving thickness of the ejecta as $\eta R/\Gamma_0$. Therefore, the comoving density of the ejecta is

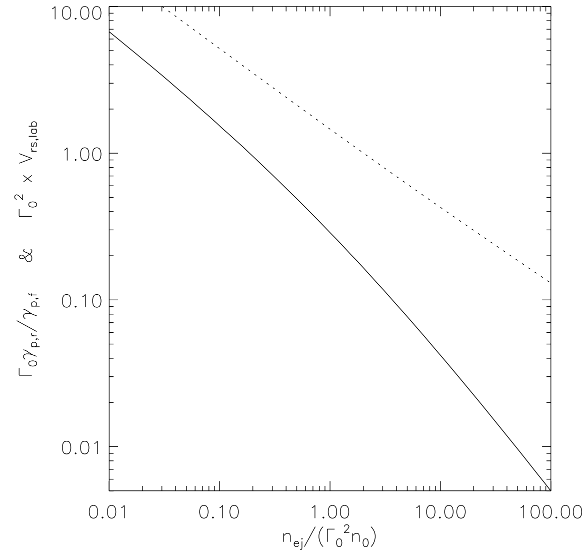

Figure 1. The solid line is the ratio of the thermal energy per proton in the reverse shock and the forward shock, $\gamma_{p,r}/\gamma_{p,f}$, as a function of n_{ej}/n (the ratio of the comoving frame density of the unshocked ejecta and of the circumburst medium). The ejecta initial Lorentz factor, Γ_0, is used to normalize both of these ratios such that the curves shown are independent of it. To a good approximation, $\Gamma_0\gamma_{p,r}/\gamma_{p,f} \simeq 0.25(n_{ej}/n_0\Gamma_0^2)^{-0.7}$. The relative velocity of the reverse shock front relative to the unshocked ejecta, as measured in the laboratory frame, $V_{rs,lab}$, is shown by the dotted line, $\Gamma_0^2 V_{rs,lab} \simeq 1.4(n_{ej}/\Gamma_0^2 n_0)^{-1/2}$.

$$n_{ej} = \frac{\mathcal{E}}{4\pi R^3 \eta m_p c^2}, \tag{3}$$

which substituted in equation (2) leads to

$$R_d = c\left[\frac{(3-s)^2\eta\mathcal{E}}{4\pi A c^2 \Gamma_0^2}\right]^{1/(3-s)}. \tag{4}$$

This result is identical to that obtained for the Blandford–McKee self-similar solution extrapolated back to R_d if we set $\eta = \frac{17}{18}$ for $s = 0$ and $\eta = \frac{9}{2}$ for $s = 2$.

From equations (3) and (4), the comoving density of the ejecta at R_d is

$$\frac{n_{ej}}{n}(R_d) = \frac{\Gamma_0^2}{(3-s)^2\eta^2}, \tag{5}$$

for $\eta \gtrsim 1$. Substituting this into equation (1), the LF of the shocked circumburst medium at R_d is

$$\Gamma_d = \frac{\Gamma_0}{[2(3-s)\eta]^{1/2}}. \tag{6}$$

From equations (4) and (6), the observer-frame deceleration timescale is

$$t_d = (1+z) f_\eta \frac{R_d}{c\Gamma_d^2} = \frac{(1+z) f_\eta}{c\Gamma_0^2}\left[\frac{(3-s)^{5-s}\eta^{4-s}\mathcal{E}}{4\pi A c^2 \Gamma_0^2}\right]^{1/(3-s)}, \tag{7}$$

where f_η is a correction factor that takes into account the difference between the arrival time $(1+z)R_d/(2c\Gamma_d^2)$ of photons emitted from the contact discontinuity[1] and that from where most of the GRB

[1] The usual factor of 2 in the denominator, corresponding to photons moving along the observer–centre direction of the explosion, is compensated by the fact that most emission arises from the gas moving at an angle Γ_d^{-1} relative to that direction.

emission arises.[2] The laboratory frame speed of the reverse shock relative to the back-end of the shell, shown in Fig. 1, is $V_{\rm rs,lab}/c \approx 1.4(3-s)\eta/\Gamma_0^2$. Thus, the time it takes for the RS to cross the shell (in the laboratory frame) is, $\eta R_{\rm d}/(\Gamma_0^2 V_{\rm rs,lab}) \approx [1.4(3-s)]^{-1} R_{\rm d}/c$. And so the RS crossing time is the same as the deceleration time to within a factor of the order of unity.

For $t > t_{\rm d}$ the LF decreases as

$$\Gamma(t) = \Gamma_{\rm d}\left(\frac{t}{t_{\rm d}}\right)^{-(3-s)/(8-2s)}. \quad (8)$$

4 FORWARD SHOCK

The comoving density behind the forward shock is, $\rho = 4\rho_0\Gamma$, and the thermal energy density is $u = 4\rho_0 c^2\Gamma^2$; where $\rho_0 = Ar^{-s}$ is the density of the medium just ahead of the shock, and Γ is the bulk LF of shocked fluid given by equation (8). A fraction $\varepsilon_{\rm e}$ of the thermal energy of the shock-heated circumburst medium is taken up by electrons. Electrons with thermal LF greater than $\gamma_{\rm i}$ are assumed to have a power-law distribution with index p, i.e. $dN_{\rm e}/d\gamma \propto \gamma^{-p}$ for $\gamma > \gamma_{\rm i}$, where $\gamma_{\rm i} = \varepsilon'_{\rm e}(m_{\rm p}/m_{\rm e})\gamma_{\rm p}$, is the minimum thermal LF of electrons; $\varepsilon'_{\rm e} = [(p-2)/(p-1)]\varepsilon_{\rm e}$ for $p > 2$ and $\gamma_{\rm p}$ is the proton thermal LF. The energy density in the magnetic field is assumed to be $\varepsilon_{B_{\rm f}} u$, and therefore the magnetic field is $B = 4\Gamma c(2\pi\varepsilon_{B_{\rm f}} Ar^{-s})^{1/2}$.

The FS synchrotron *injection* frequency, $\nu_{\rm if}$ and the flux at the peak of the F_ν spectrum, are

$$\nu_{\rm if}(t) = \frac{qB\gamma_{\rm i}^2\Gamma}{2\pi m_{\rm e}c(1+z)} = \frac{4q\varepsilon_{\rm e}'^2\varepsilon_{\rm Bf}^{1/2}m_{\rm p}^2A^{1/2}\Gamma_{\rm d}^{4-s}}{\sqrt{2\pi}m_{\rm e}^3(1+z)}\left[\frac{4(4-s)ct_{\rm d}}{1+z}\right]^{-s/2}\left(\frac{t}{t_{\rm d}}\right)^{-3/2}, \quad (9)$$

$$F_{\rm p,f}(t) = \frac{N_{\rm e}\varepsilon'_{\rm p}\Gamma}{d_L'^2} = \frac{4(6\pi)^{1/2}q^3A^{3/2}\varepsilon_{\rm Bf}^{1/2}\Gamma_{\rm d}^{8-3s}}{m_{\rm p}m_{\rm e}c(3-s)d_L'^2}\left[\frac{4(4-s)ct_{\rm d}}{1+z}\right]^{3(2-s)/2} \times\left(\frac{t}{t_{\rm d}}\right)^{-s/(8-2s)}, \quad (10)$$

where q and $m_{\rm e}$ are the electron charge and mass, respectively, $m_{\rm p}$ is the proton mass and $d'_L = D_L/\sqrt{1+z}$, with D_L being the luminosity distance, $N_{\rm e} = AR^{3-s}/(3-s)$ is the number of electrons per unit solid angle behind the shock and $\varepsilon'_{\rm p} = 3^{1/2}q^3B/m_{\rm e}c^2$ is the power per unit frequency per electron, in the comoving frame, at the peak of the synchrotron spectrum.

The synchrotron injection frequency for the cases of $s = 0$ and 2 are written out explicitly for ease of application later on

$$\nu_{\rm if}(t) = \varepsilon_{\rm e}'^2\varepsilon_{\rm Bf,-4}^{1/2}(t/t_{\rm d})^{-3/2} \times\begin{cases}3.7\times10^{18}n_0^{1/2}\Gamma_{\rm d,2}^4(1+z)^{-1}\ {\rm Hz} & s=0\\ 1.7\times10^{21}A_*^{1/2}\Gamma_{\rm d,2}^2t_{\rm d}^{-1}\ {\rm Hz} & s=2,\end{cases} \quad (11)$$

where $A_* = A/(5\times10^{11})$ g cm^{-1}, $t_{\rm d}$ is the deceleration time in seconds, and an integer subscript n on a variable X, X_n, means $X/10^n$.

[2] For instance, if the burst is FS synchrotron emission from higher-energy electrons in a fast cooling regime, then the γ-ray emission arises from the shocked gas immediately behind the FS and $f_\eta = \frac{1}{4}$. At the other extreme, when the burst arises from fast cooling electrons located immediately behind the reverse shock, it can be shown that $f_\eta \simeq \frac{1}{2}\sqrt{\eta/(3-s)}$ for $\eta \gg 1$.

The flux at the peak of the synchrotron spectrum for $s = 0$ and 2 is

$$F_{\rm p,f}(t) = \varepsilon_{\rm Bf,-4}^{1/2}\Gamma_{\rm d,2}^2 \times\begin{cases}5.5\times10^{-7}n_0^{3/2}\Gamma_{\rm d,2}^6t_{\rm d}^3\ {\rm mJy} & s=0\\ 1.2\times10^3A_*^{3/2}(t/t_{\rm d})^{-1/2}\ {\rm mJy} & s=2.\end{cases} \quad (12)$$

In the derivation of the above equation we have set $z = 1$, which corresponds to the redshift of GRB 021211.

The FS synchrotron self-absorption frequency ($\nu_{\rm Af}$), obtained by equating the intensity at $\nu_{\rm Af}$ to $2m_{\rm e}\gamma_{\rm if}\nu_{\rm Af}^2$, is given by

$$\nu_{\rm Af}^2\left(\frac{\nu_{\rm if}}{\nu_{\rm Af}}\right)^\alpha = \frac{(6\pi\varepsilon_B)^{1/2}q^3A^{3/2}\Gamma_{\rm d}^{4-3s}(4t_{\rm d})^{(2-3s)/2}}{8(3-s)m_{\rm e}m_{\rm p}^2\varepsilon'_{\rm e}(1+z)^{(6-3s)/2}c^{3s/2}} \times\left(\frac{t}{t_{\rm d}}\right)^{-(s+4)/(8-2s)}, \quad (13)$$

where α depends on the relative location of $\nu_{\rm Af}$ with respect with $\nu_{\rm if}$ and the cooling frequency $\nu_{\rm cf}$; for $\nu_{\rm cf} > \nu_{\rm if} > \nu_{\rm Af}$, $\alpha = \frac{1}{3}$, and $\alpha = p/2$ if $\nu_{\rm if} < \nu_{\rm Af} < \nu_{\rm cf}$.

We make use of the optical *R*-band flux of the afterglow 021211 at $t \geqslant 11$ min to constrain the density, magnetic field parameter and the Lorentz factor at deceleration. According to Li et al. (2003) the contributions from the reverse and forward shocks to the observed *R*-band flux are equal at this time, each being approximately 0.2 mJy. Therefore, the FS peak flux at 11 min is greater than 0.2 mJy. We will consider the peak flux to be $0.2A_{\rm f}$ mJy, with $A_{\rm f} > 1$. The *R*-band light curve is monotonically declining from 11 min to 10 d as a pure power law. Thus, the frequency of the peak of the spectrum at 11 min is less than the *R*-band frequency (4.7×10^{14} Hz). We assume that the peak frequency at 11 min is a factor of A_ν smaller than the *R*-band frequency. Therefore, for a time-independent parameter $\varepsilon_{\rm Bf}$, the synchrotron peak frequency as a function of time is

$$\nu_{\rm if} = 37t^{-3/2}A_\nu^{-1}\ {\rm keV}. \quad (14)$$

Note that $A_{\rm f}$ and A_ν are related by $A_{\rm f} = A_\nu^{(p-1)/2}$, if the cooling frequency ($\nu_{\rm c}$) is above the R band at 11 min, and $A_{\rm f} = A_\nu^{p/2}$ if $\nu_{\rm c}$ is below the R band.

4.1 Parameters for a uniform circumburst medium

Using equation (7) the bulk LF at deceleration time, for $s = 0$, is

$$\Gamma_{\rm d,2} = 3.8\left(\frac{\mathcal{E}_{52}}{n_0}\right)^{1/8}\left[\frac{f_\eta(1+z)}{t_{\rm d}}\right]^{3/8}, \quad (15)$$

where n is the density of the uniform circumburst medium, in cm^{-3}, $f_\eta = \max\{1, 2\sqrt{\eta}/3\}$ (see footnote) and an integer subscript on a variable X_n means $X/10^n$, with X in cgs units.

Using equation (15) to eliminate $\Gamma_{\rm d}$ from equation (12), the peak flux at 11 min implies that

$$n_0^{1/2}\mathcal{E}_{52}\varepsilon_{\rm Bf,-4}^{1/2} = A_{\rm f}f_\eta^{-3}. \quad (16)$$

Substituting the peak frequency at 11 min (equation 14) in equation (11) and using equation (15), we obtain

$$\varepsilon_{B_{\rm f}}(t = 11\ {\rm min}) = 6.4\times10^{-5}A_\nu^{-2}\mathcal{E}_{52}^{-1}\varepsilon_{e-1}'^{-4}f_\eta^{-3}. \quad (17)$$

Combining equations (15)–(17) we find

$$\Gamma_{\rm d} \approx 150(A_\nu A_{\rm f})^{-1/4}f_\eta^{3/4}\mathcal{E}_{52}^{1/4}\varepsilon_{\rm e}'^{-1/2}t_{\rm d}^{-3/8}, \quad (18)$$

$$n = 1.5(A_\nu A_{\rm f})^2\mathcal{E}_{52}^{-1}f_\eta^{-3}\varepsilon_{e_{-1}}'^4\ {\rm cm}^{-3}. \quad (19)$$

4.2 Parameters for an r^{-2} external medium

For $s = 2$, equation (7) gives that

$$\Gamma_{d,2} = 0.53 \left[\frac{(1+z)\mathcal{E}_{52} f_\eta}{A_* t_d}\right]^{1/4}, \quad (20)$$

where $f_\eta = \max(1, \sqrt{2\eta}/3)$. Since the peak flux at 11 min is 0.2 A_f mJy, the FS peak flux (for constant ε_{Bf}) at an earlier time is

$$F_{p,f} = 5.4 A_f t^{-1/2}\ \mathrm{mJy}. \quad (21)$$

Substituting this in equation (12) and using equation (20) leads to

$$A_* \mathcal{E}_{52}^{1/2} \varepsilon_{Bf,-4}^{1/2} = 1.1 \times 10^{-2} A_f f_\eta^{-1/2}. \quad (22)$$

For $s = 2$, equations (11) and (14) yield

$$\varepsilon_{B_f}(t = 11\ \mathrm{min}) = 1.7 \times 10^{-8} A_\nu^{-2} \mathcal{E}_{52}^{-1} \varepsilon_{e-1}^{\prime -4} f_\eta^{-1}. \quad (23)$$

Substituting equation (23) in (22), we obtain

$$A_* = 0.90 \varepsilon_e^{\prime 2}(A_\nu A_f), \quad (24)$$

which, together with equation (20), gives the LF at deceleration

$$\Gamma_d = 70 \mathcal{E}_{52}^{1/4} t_d^{-1/4} f_\eta^{1/4} \varepsilon_e^{\prime -1/2} (A_\nu A_f)^{-1/4}. \quad (25)$$

We see from these equations that for $s = 2$, A_ν can be as large as 10–20, and yet give acceptable values for various parameters.

5 REVERSE SHOCK

The emission from reverse shock in gamma-ray bursts is discussed by various authors (e.g. Panaitescu & Mészáros 1998; Sari & Piran 1999; Kobayashi 2000). A particularly important parameter that determines the behaviour of RS is the thickness of the ejecta shell that carries the relativistic energy of the explosion. We have parametrized the ejecta thickness as $\eta R/\Gamma_0^2$ in the laboratory frame; for a shell where the thickness is dominated by expansion at the deceleration radius we expect $\eta \sim 1$, otherwise the thickness is determined by the duration of the central engine, and η could be much larger than unity at t_d. We calculate RS emission for a range of η between 0.5 and 10. Fortunately, the main conclusions of this work for GRB 021211 remain unchanged even for a larger range of η.

At the deceleration radius R_d, the ratio of the thermal energy of protons in the reverse shock region, $\gamma_{p,r}$, to that in the FS, $\gamma_{p,f}$, is (see Fig. 1)

$$\frac{\gamma_{p,r}}{\gamma_{p,f}} \approx \frac{1}{4\Gamma_0}\left(\frac{n_{ej}}{\Gamma_0^2 n}\right)^{-0.7} \approx \frac{[(3-s)\eta]^{1.4}}{4\Gamma_0} = \frac{[(3-s)\eta]^{0.9}}{\sqrt{32}\Gamma_d}. \quad (26)$$

The first part in the above equation is valid only for $0.01 \lesssim n_{ej}/\Gamma_0^2 n \lesssim 100$; for $n_{ej}/\Gamma_0^2 n \ll 0.01$, it can be shown that $\gamma_{p,r}/\gamma_{p,f} \simeq (n_{ej}/n)^{-1/2}$. In deriving the second part of this equation we made use of (5) for the density of the ejecta at $R_d - n_{ej}(R_d)$. It should be noted that the thermal energy per proton in RS is $\sim m_p c^2 \eta^{0.9}/32^{1/2}$, and so protons are not heated to a relativistic temperature in the reverse shock as long as $\eta \ggg 1$.

The pressure continuity across the contact discontinuity surface, which separates forward and reverse shocks, implies that the magnetic field strength in RS and FS are equal, provided that ε_B is the same behind both shocks. However, it is possible that the magnetic field parameter in the RS (ε_{Br}) is different from that in the FS (ε_{Bf}), due to the different strengths of the two shocks or if the ejecta were initially magnetized. Then the synchrotron peak frequency in the RS is

$$\nu_{ir}(t_d) = \nu_{if}(t_d)\left(\frac{\varepsilon_{Br}}{\varepsilon_{Bf}}\right)^{1/2}\left(\frac{\gamma_{p,r}}{\gamma_{p,f}}\right)^2_{t_d} = \nu_{if}(t_d)\frac{[(3-s)\eta]^{1.8}}{32\Gamma_d^2}\left(\frac{\varepsilon_{Br}}{\varepsilon_{Bf}}\right)^{1/2}. \quad (27)$$

This can be written out explicitly as follows:

$$\nu_{ir}(t_d) = \frac{q m_p^2 \varepsilon_{Br}^{1/2} \varepsilon_e^{\prime 2} A^{1/2} R_d^{-s/2} \Gamma_d^2 [(3-s)\eta]^{1.8}}{(128\pi)^{1/2}(1+z) m_e^3} \quad (28)$$

or

$$\nu_{ir}(t_d) = \varepsilon_{Br,-4}^{1/2} \varepsilon_e^{\prime 3} (A_\nu A_f)^{1/2} \eta^{1.8} \times \begin{cases} 1.1 \times 10^{16} t_d^{-3/4}\ \mathrm{Hz} & s = 0 \\ 5.1 \times 10^{15} t_d^{-1}\ \mathrm{Hz} & s = 2. \end{cases} \quad (29)$$

In deriving this last equation we made use of equations (18), (19), (24) and (25) for the circumburst density and LF at deceleration.

Since the FS and RS region are moving at same LF, at deceleration, the RS peak synchrotron flux is equal to the FS peak flux times the ratio of number of electrons in the ejecta to the swept-up electrons in the surrounding medium; this ratio is equal to $\Gamma_0/(3-s)\eta = [2/(3-s)\eta]^{1/2}\Gamma_d$. Thus, the RS peak flux is

$$F_{p,r}(t_d) = F_{p,f}(t_d)\left[\frac{2(\varepsilon_{Br}/\varepsilon_{Bf})}{(3-s)\eta}\right]^{1/2}\Gamma_d \quad (30)$$

or

$$F_{p,r}(t_d) = \frac{(3\varepsilon_{Br} A)^{1/2} q^3 \mathcal{E}(1+z)^{s/2}}{m_e m_p c^3 d_L^{\prime 2} \Gamma_d^{s-1} (4ct_d)^{s/2} [\pi(3-s)\eta]^{1/2}}. \quad (31)$$

Using (18), (19), (24) and (25) this equation reduces to

$$F_{p,r}(t_d) = \varepsilon_{Br,-4}^{1/2} \varepsilon_e^{\prime 3/2} (A_\nu A_f)^{3/4} \mathcal{E}_{52}^{3/4} \eta^{-1/2} \times \begin{cases} 2.9 \times 10^3 t_d^{-3/8}\ \mathrm{mJy} & s = 0 \\ 3.8 \times 10^4 t_d^{-3/4}\ \mathrm{mJy} & s = 2. \end{cases} \quad (32)$$

The RS synchrotron self-absorption frequency is

$$\nu_{Ar}^2(t_d)\left(\frac{\nu_{ir}}{\nu_{Ar}}\right)^\alpha = \frac{q^3 E\left[6\pi\varepsilon_B A(1+z)^s\right]^{1/2}}{8\pi m_e m_p^2 c^3 \varepsilon_e^\prime [(3-s)\eta]^{1.4} (4ct_d)^{(s+4)/2} \Gamma_d^{s+2}}, \quad (33)$$

where $\alpha = \frac{1}{3}$ if $\nu_{ir} > \nu_{Ar}$, and $p/2$ otherwise. Using equations (18), (19), (24) and (25) this can be rewritten as

$$\nu_{Ar}(t_d)\left(\frac{\nu_{ir}}{\nu_{Ar}}\right)^{\alpha/2} = \varepsilon_{Br,-4}^{1/4} \varepsilon_e^\prime (A_\nu A_f)^{3/4} \eta^{-0.7} \times \begin{cases} 5.5 \times 10^{13} t_d^{-5/8}\ \mathrm{Hz} & s = 0 \\ 1.1 \times 10^{15} t_d^{-1}\ \mathrm{Hz} & s = 2. \end{cases} \quad (34)$$

The time dependence of ν_{ir} and $F_{p,r}$ is determined by the evolution of the magnetic field and the electron thermal energy in the reverse shock. Electrons in the ejecta cease to be heated after the passage of the RS, and their energy decreases with time as a result of adiabatic expansion. If electrons continue to exchange energy with protons, and the fraction of thermal energy in electrons, ε_e, is time independent, then electron thermal LF decreases as

$$\gamma_e \propto (R^2 \delta R)^{-(2-\varepsilon_e)/3} \propto t^{-2(2-\varepsilon_e)/3(4-s)}, \quad (35)$$

where δR is the comoving shell thickness which is a weak function of time for sub-relativistic or mildly relativistic RS, and R, the radius of the ejecta, increases with time as $t^{1/(4-s)}$; $\varepsilon_e = 1$ if electrons and protons are decoupled.

The magnetic field, frozen in the ejecta, decreases as $B' \propto (R\delta R)^{-1} \propto t^{-1/(4-s)}$ if the field is transverse; a longitudinal field decreases as $B' \propto R^{-2} \propto t^{-2/(4-s)}$, therefore any non-zero transverse field will become the dominant component at large distances.

Thus, after the reverse shock has crossed the ejecta, the synchrotron injection frequency and the peak flux decrease as

$$\nu_{\rm ir} \propto B'\gamma_{\rm e}^2\Gamma \propto t^{-(31-3s-8\varepsilon_{\rm e})/6(4-s)},$$
$$F_{\rm p,r} \propto N_{\rm e}B'\Gamma \propto N_{\rm e}t^{-(5-s)/2(4-s)}, \tag{36}$$

where $N_{\rm e}$ is the total number of 'radiating' electrons in the ejecta. The cooling frequency (where radiative and adiabatic loss time-scales are equal) decreases at the same rate as $\nu_{\rm ir}$. Above the cooling frequency, the electron distribution develops a sharp cut-off due to the fast cooling of the higher-energy electrons and the lack of a shock injecting fresh electrons.

For the electron index p required by the $t^{-0.82}$ decay observed in the late optical (FS emission), the above equations lead to a decay of the early optical afterglow (RS emission), which is shallower than observed ($t^{-1.82}$). This may be due to several departures from the standard model. The number of electrons radiating in an observer band might have a non-trivial time dependence if the magnetic field is not constant across the ejecta – electrons in a region of higher magnetic field lose energy at a higher rate and the frequency at which they radiate drops below the observed band sooner than for electrons in a region of lower field. Together with the uncertain evolution of $\gamma_{\rm e}$ (which depends on the coupling between electrons and protons) and the unknown energy density and LF structure of the ejecta, this makes it difficult to calculate the (power-law) decay of the RS flux reliably.

In order to explain the decay of the early optical emission of GRB 021211, we determine from the observed light-curve slope the decay of synchrotron frequency – which depends on both B' and $\gamma_{\rm e}$, so its time dependence is more uncertain than that of the peak flux, which depends only on B'. Let us consider the time dependence for injection frequency and peak flux to be $t^{-\alpha_\nu}$ and $t^{-\alpha_{\rm f}}$, respectively. The flux above the synchrotron peak decays as $t^{-[\alpha_{\rm f}+(p-1)\alpha_\nu/2]}$, where p is the electron energy power-law index. We take $\alpha_{\rm f}$ to be as given in equation (36), but make allowance for a small deviation in its value. Thus, the observed decay for GRB 021211, $t^{-1.8}$, is used to determine α_ν. With α_ν and $\alpha_{\rm f}$ thus known, we find the time dependence of B' and $\gamma_{\rm e}$,

$$B' \propto t^{-\alpha_{\rm f}+(3-s)/(8-2s)}, \qquad \gamma_{\rm e} \propto t^{-(\alpha_\nu-\alpha_{\rm f})/2}, \tag{37}$$

which are used to calculate the absorption and cooling frequencies and the flux as a function of time.

6 COMPTON PARAMETER AND COOLING FREQUENCY

In this section we calculate the cooling frequency at deceleration; its value at later times in the reverse and forward shocks follows from the adiabatic losses behind the reverse shock and the standard results of forward shock afterglow theory, respectively.

The comoving frame time-scale for an electron of energy $m_{\rm e}c^2\gamma_{\rm e}$ to cool (as a result of synchrotron and inverse Compton emission) is

$$t'_{\rm c} = \frac{6\pi m_{\rm e}c}{\sigma_{\rm T}B'^2\gamma_{\rm e}(1+Y)} = \frac{3m_{\rm e}R_{\rm d}^s}{16\sigma_{\rm T}c\varepsilon_B\gamma_{\rm e}\Gamma_{\rm d}^2A(1+Y)}, \tag{38}$$

where Y is the Compton Y parameter, a prime denotes a comoving quantity and the cooling is considered at the deceleration time. At deceleration, when $t'_{\rm c} = 4t_{\rm d}\Gamma_{\rm d}/(1+z)$, the electron cooling LF, $\gamma_{\rm c}$, defined by the equality of the radiative and dynamical time-scales, is

$$\gamma_{\rm c}(t_{\rm d}) = \frac{3\pi m_{\rm e}c(1+z)}{2\sigma_{\rm T}B'^2t_{\rm d}\Gamma_{\rm d}(1+Y)} = \frac{3(1+z)^{1-s}m_{\rm e}\Gamma_{\rm d}^{2s-3}}{16\sigma_{\rm T}\varepsilon_BA(4ct_{\rm d})^{1-s}(1+Y)}. \tag{39}$$

Substituting for A and $\Gamma_{\rm d}$ from equations (18), (19), (24) and (25) we obtain

$$\gamma_{\rm c}(t_{\rm d}) = \frac{\mathcal{E}_{52}^{1/4}}{\varepsilon_{B,-4}\varepsilon_{\rm e}'^{5/2}(A_\nu A_{\rm f})^{5/4}(1+Y)} \times \begin{cases} 510t_{\rm d}^{1/8} & s=0 \\ 22t_{\rm d}^{3/4} & s=2. \end{cases} \tag{40}$$

The cooling frequency $\nu_{\rm c}$, defined as the synchrotron frequency for electrons with LF $\gamma_{\rm c}$, is

$$\nu_{\rm c}(t_{\rm d}) = \frac{qB'\gamma_{\rm c}^2\Gamma_{\rm d}}{2\pi m_{\rm e}c(1+z)} = \frac{6.1\times10^{-5}c^2\left(4ct_{\rm d}\Gamma_{\rm d}^2\right)^{(3s-4)/2}}{(1+z)^{1.5s-1}(A\varepsilon_{B,-4})^{3/2}(1+Y)^2}\ {\rm Hz}, \tag{41}$$

which can be rewritten by substituting for A and $\Gamma_{\rm d}$,

$$\nu_{\rm c}(t_{\rm d}) = \frac{\mathcal{E}_{52}^{1/2}}{\varepsilon_{B,-4}^{3/2}\varepsilon_{\rm e}'^4(A_\nu A_{\rm f})^2(1+Y)^2} \times \begin{cases} 2\times10^{15}(1+z)t_{\rm d}^{-1/2}\ {\rm Hz} & s=0 \\ 9\times10^{13}(1+z)^{-2}t_{\rm d}^{1/2}\ {\rm Hz} & s=2. \end{cases} \tag{42}$$

The cooling frequencies in the reverse and forward shock regions are calculated from this equation by substituting appropriate values for ε_B and Y corresponding to each region.

For fast cooling electrons, $\nu_{\rm A} < \nu_{\rm c} < \nu_{\rm i}$, the Compton parameter takes a simple form

$$Y \simeq \left(\frac{\varepsilon_{\rm e}}{\varepsilon_B}\right)^{1/2}. \tag{43}$$

For $\nu_{\rm A} < \nu_{\rm i} < \nu_{\rm c}$, the Compton parameter is $Y = \tau\overline{\gamma_{\rm e}^2}$, where $\overline{\gamma_{\rm e}^2}$ is the mean squared electron LF. For $2 < p < 3$

$$\overline{\gamma_{\rm e}^2} = \frac{(p-1)}{(p-2)(3-p)}\gamma_{\rm i}^2\left(\frac{\gamma_{\rm c}}{\gamma_{\rm i}}\right)^{3-p}, \tag{44}$$

where $m_{\rm e}c^2\gamma_{\rm i}$ is the minimum thermal energy of shock-heated electrons and τ is the optical depth to Thomson scattering.

The electron column density in the ejecta, at the deceleration radius, assuming that the ejecta consist only of protons and electrons, i.e. there are no pairs, is

$$N_{\rm e,r} = \frac{\mathcal{E}}{4\pi R_{\rm d}^2\Gamma_0m_{\rm p}c^2} = \frac{(1+z)^2\mathcal{E}}{64\pi\sqrt{2(3-s)}\eta m_{\rm p}c^4t_{\rm d}^2\Gamma_{\rm d}^5}. \tag{45}$$

The optical depth of the ejecta to Thomson scattering is

$$\tau_r(t_{\rm d}) = \sigma_{\rm T}N_{\rm e,r} = 1.7\times10^{-3}\frac{(1+z)^2\mathcal{E}_{52}}{\sqrt{(3-s)}\eta t_{\rm d}^2\Gamma_{\rm d,2}^5}. \tag{46}$$

Substituting equation (40) into (44) and making use of equations (26) and (46), we find the Compton Y parameter in the reverse shock region

$$Y(1+Y)^{3-p}(t_{\rm d}) = \frac{(p-1)\varepsilon_{\rm Br,-4}^{p-3}\varepsilon_{\rm e}'^{(7p-12)/2}(A_\nu A_{\rm f})^{5(p-2)/4}\eta^{0.9p-1.4}}{(p-2)(3-p)(m_{\rm e}/m_{\rm p})^{p-1}32^{(p-1)/2}\mathcal{E}_{52}^{(p-2)/4}} \times \begin{cases} 2.8\times10^4(190^{-p})t_{\rm d}^{-(p-2)/8} & s=0 \\ 6.4\times10^2(22^{-p})t_{\rm d}^{-3(p-2)/4} & s=2. \end{cases} \tag{47}$$

The optical depth to Thomson scattering in the forward shock at the deceleration time is

$$\tau_f(t_d) = \frac{\sigma_T A R_d^{1-s}}{(3-s)m_p} = \frac{\varepsilon_e'^{3}(A_f A_\nu)^{3/2}}{\mathcal{E}_{52}^{1/2}} \times \begin{cases} 8.9\times10^{-6} t_d^{1/4}(1+z)^{-1} & s=0 \\ 1.7\times10^{-4} t_d^{-1/2}(1+z) & s=2, \end{cases} \quad (48)$$

where $R_d = 4ct_d\Gamma_d^2/(1+z)$ is the deceleration radius and the last equality was obtained by making use of equations (18), (19), (24) and (25) to eliminate Γ_d and n. Substituting into $Y = \tau_f\overline{\gamma_e^2}$ equations (40), (44), (48) and the expression for the injection LF of electrons in the forward shock at t_d, $\gamma_i = (m_p/m_e)\varepsilon_e'\Gamma_d$, we obtain

$$Y(1+Y)^{3-p}(t_d) = \frac{(p-1)\varepsilon_{Bf,-4}^{p-3}\varepsilon_e'^{(7p-11)/2}(A_f A_\nu)^{(5p-9)/4}\Gamma_d^{p-1}}{(3-p)(p-2)(m_e/m_p)^{p-1}\mathcal{E}_{52}^{(p-1)/4}} \times \begin{cases} 4.5\times10^{-6}(513^{3-p}) t_d^{(5-p)/8} & s=0 \\ 7.4\times10^{-4}(22^{3-p}) t_d^{(7-3p)/4} & s=2. \end{cases} \quad (49)$$

When $\nu_A > \min\{\nu_c, \nu_i\}$, the synchrotron photon flux that is scattered by an electron is diminished by self-absorption and ν_A and ν_c have to be determined by solving a set of coupled equations, as described in Panaitescu & Mészáros (2000). Some of the cases considered for GRB 021211 fall in this more complicated regime, and all of the numerical results presented in this paper are obtained by determining ν_A and ν_c numerically, in a self-consistent manner.

7 UNIFORM DENSITY CIRCUMBURST MEDIUM ($s = 0$)

We apply the results of the last three sections to a systematic analysis of γ-ray, optical and radio observations for GRB 021211 and determine models that are consistent with all data. In this section, we discuss a uniform density circumburst medium ($s = 0$). A medium carved out by the wind of the progenitor ($s = 2$) is the subject of the following section.

7.1 Optical emission from reverse shock

At deceleration, the RS synchrotron injection frequency is a factor of $(\gamma_{p,f}/\gamma_{p,r})^2$ smaller compared with the peak frequency of the FS emission, if ε_B is the same in the reverse and forward shocks. Thus, if ε_{Bf} is constant in time, equations (14), (18) and (27) give that the synchrotron injection frequency in the RS is $0.37\eta^{1.8}\varepsilon_e'(\varepsilon_{Br}/\varepsilon_{Bf})^{1/2}$ eV. This suggests that the RS flux in the optical band decreases with time for $t > t_d$. The extrapolation of the observed flux of 7.2 mJy at 90 s, with a power-law decline of $t^{-1.8}$, gives an R-band flux at 5 s of 1.3 Jy or 8.5 mag. Thus the afterglow of GRB 021211 could have been as bright as that of GRB 990123 during and shortly after the burst.

The injection frequency in RS for $s = 0$ declines with the observer time approximately as $t^{-5/4}$, and the cooling frequency also declines as $t^{-5/4}$ or faster. After the passage of the reverse shock, which takes place on the deceleration time-scale of a few seconds for GRB 021211, electrons are no longer accelerated and there is no emission from RS at a frequency greater than the cooling frequency (ν_{cr}). The $t^{-1.8}$ decay of the optical light curve, observed until 11 min, suggests that the optical RS emission lasts for at least 11 min, therefore ν_{cr} at deceleration should be $\gtrsim 10^{17}$ Hz.

The inverse Compton parameter and the cooling frequency are determined from equations (42) and (47). For $p = 2.5$ these quantities are

$$Y(1+Y)^{1/2}(t_d) = 2\times10^3\varepsilon_e'^{2.75}\varepsilon_{Br,-4}^{-1/2}\eta^{0.85}A_\nu^{35/32}\mathcal{E}_{52}^{-1/8}t_d^{-1/16}, \quad (50)$$

$$\nu_{cr}(t_d) = 1.5\times10^{11}\frac{\mathcal{E}_{52}^{1/2}}{\varepsilon_e'^{7.7}\varepsilon_{Br,-4}^{0.83}\eta^{1.1}A_\nu^5 t_d^{2/5}}\ \mathrm{Hz}, \quad (51)$$

if $Y \gtrsim 1$. For $Y \ll 1$ the cooling frequency is obtained by setting $Y = 0$ in equation (42).

The above requirement that $\nu_{cr}(t_d) > 10^{17}$ Hz provides an upper limit on ε_e':

$$\varepsilon_e' \lesssim \frac{0.18\mathcal{E}_{52}^{1/15.4}}{\varepsilon_{Br,-4}^{1/9}A_\nu^{2/3}\eta^{1/7}t_d^{1/20}}. \quad (52)$$

Substituting this into equations (29) and (32), we find the injection frequency and peak flux from the RS

$$\nu_{ir}(t_d) \lesssim 6\times10^{13}\varepsilon_{Br,-4}^{1/6}\mathcal{E}_{52}^{1/5.1}A_\nu^{-1.1}\eta^{1.37}t_d^{-0.9}\ \mathrm{Hz}, \quad (53)$$

$$F_{p,r}(t_d) \lesssim 220\,\varepsilon_{Br,-4}^{1/3}\mathcal{E}_{52}^{0.85}A_\nu^{7/20}\eta^{-0.7}t_d^{-0.45}\ \mathrm{mJy}. \quad (54)$$

When $\nu_{ir}(t_d)$ is below the optical domain, the flux in the R band ($\nu_R \approx 4.9\times10^{14}$ Hz) at deceleration time is

$$F_{\nu_R}(t_d) \lesssim 46\varepsilon_{Br,-4}^{0.46}\mathcal{E}_{52}A_\nu^{-7/16}\eta^{0.3}t_d^{-1.1}\ \mathrm{mJy}, \quad (55)$$

whereas the flux in the R band at 90 s is $F_{\nu_R}(t = 90\ \mathrm{s}) = F_{\nu_R}(t_d)(90\ \mathrm{s}/t_d)^{-1.8}$. The above equations are applicable when the synchrotron self-absorption frequency is less than ν_R, which is indeed the case (see equation 34).

Thus the R-band flux at 90 s is $0.014\varepsilon_{Br,-4}^{0.46}\mathcal{E}_{52}A_\nu^{-7/16}\eta^{0.3}t_d^{0.7}$ mJy. The observed R-band flux of 7.2 mJy requires $\varepsilon_{Br} \sim 10^{-1}$, $\mathcal{E}_{52} \sim 20$ and $A_\nu \sim \eta$. Fig. 2 shows the allowed parameter space, which satisfies the R-band flux at $t \geqslant 90$ s. Note that $\varepsilon_{Br}/\varepsilon_{Bf}(t = 11\ \mathrm{min}) \gtrsim 10^3$, a result consistent with the analytical calculation presented above.

Fox et al. (2003) reported that the flux at 8.5 GHz, 0.1 d after the burst, was less than 110 μJy. This frequency is above the self-absorption frequency and the flux from RS is a few times larger than this upper limit for the parameter space in Fig. 2. At the small Galactic latitude of GRB 021211, the transition frequency for interstellar scintillation, from the diffractive to the refractive regime, is $\nu_0 \sim 8$ GHz. Thus taking into account the small source size at 0.1 d, it follows that the 8.5-GHz afterglow flux could be modulated by approximately a factor of 2 due to scintillation, which can explain the low radio flux upper limit reported by Fox et al. (2003). The radio flux at 0.1 d can also be reduced if the magnetic field in the ejecta is not uniform as considered here. We note that the radio flux would exceed the observational limit by almost an order of magnitude if the time for RS crossing were taken to be 30 s, almost independent of the details of the RS model, which suggests that the shock crossing time is approximately equal to the burst duration of 2–4 s.

7.2 γ-ray emission

The injection frequency in FS at the deceleration time ($t_d = 2$s) is 13 A_ν^{-1} keV (see equation 14), and the peak flux is $0.2A_f$ mJy. To explain the early optical afterglow requires A_ν to be of the order of a few or larger (see Fig. 2 and the discussion in the previous subsection), therefore the injection frequency and the peak flux in FS at t_d are ∼5 keV and 0.4 mJy, respectively. The observed peak flux

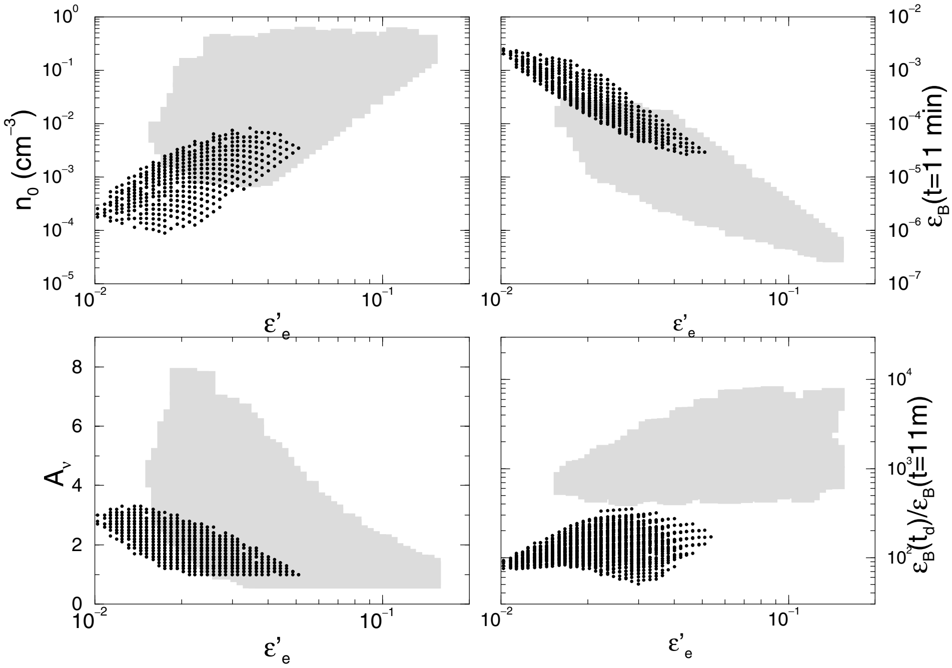

Figure 2. Grey area: parameter space (and derived quantities) for a *homogeneous* external medium allowed by the observed *R*-band flux from the reverse shock at 90 s and from the forward shock at 11 min, but not including the γ-ray flux during the burst. Black dots show the parameter space allowed for the observed gamma-ray flux to arise in forward shock as synchrotron emission; inverse Compton emission in FS or RS cannot account for the observed γ-ray spectrum. The top left-hand panel shows the allowed density for the circumburst medium (n) and ε'_e (which gives the minimum LF of shock heated electrons). The top right-hand panel shows the allowed value for the magnetic field parameter ε_B in the forward shock at 11 min. The lower left-hand panel shows A_ν, a parameter that specifies the peak of the synchrotron spectrum at 11 min (the peak frequency is $5 \times 10^{14}/A_\nu$ Hz). The lower right-hand panel shows the ratio of ε_B in the RS at deceleration to that in the FS at 11 min (grey region), and the ratio of ε_B in the FS at deceleration and at 11 min. Note that ε_B in RS is larger by a factor of approximately 10^3 compared with the value in FS at 11 min, and ε_B in FS at deceleration is larger than at 11 min by a factor of approximately 10^2. $\mathcal{E}_{52} = 30$, $t_d = 3$s, $p = 2.5$ and $z = 1.0$ for all calculations; $p = 2.2$ gives very similar results.

during the GRB is ~4 mJy, approximately an order of magnitude larger than predicted by the extrapolation of the optical data at 11 min. The peak of νF_ν, at ~50 keV (Crew et al. 2003), is also approximately an order of magnitude larger than the synchrotron peak frequency.

We consider whether synchrotron self-Compton scattering in the reverse or the forward shock might explain the gamma-ray emission. The peak of νF_ν for inverse Compton scattered synchrotron photons occurs at a frequency of $\max\{\gamma_i^2, \gamma_c^2\} \times \max\{\nu_i, \nu_c\}$ (see Panaitescu & Mészáros 2000). For the reverse shock of GRB 021211, the parameters determined in Section 7.1 lead to $\nu_i(t_d) < \nu_c(t_d)$, $\nu_c \sim 1$ keV, and $\gamma_c \sim 3 \times 10^2$, therefore the IC power peaks at ~100 MeV, or three orders of magnitude above the observed peak; the IC flux at 50 keV is approximately 0.1 mJy. For the forward shock, $\nu_i \sim 5$ keV and $\gamma_i \sim 10^4$, and thus the IC spectrum peaks at an energy of $\gtrsim$0.5 TeV; the flux at this energy is smaller than the upper limit provided by Milagro (McEnery et al. 2002).

Having eliminated the synchrotron self-Compton process as an explanation for the γ-ray emission from GRB 02121, we turn to synchrotron emission from the reverse or the forward shock as a possible GRB mechanism.

The synchrotron emission from RS can have $\nu_c \sim 50$ keV provided that $\varepsilon'_e \sim 0.04$. The flux at 50 keV can be calculated directly from the observed optical *R*-band flux and is estimated to be approximately 4 mJy – consistent with the observed γ-ray flux. This would have been a very economical and elegant explanation for all the observations for 021211 from γ-ray to radio frequencies. Unfortunately, this possibility is ruled out by the observed spectral power-law index of 0.24 below the 50-keV peak (Crew et al. 2003), as the RS synchrotron model predicts a spectral power-law index of $-(p-1)/2 \sim -0.5$.

As discussed above, synchrotron emission from the forward shock cannot account for the gamma-ray observations if ε_B in the FS as the deceleration is the same as at 11 min. Our goal is to explain the burst peak flux of 4 mJy and the peak frequency of 50 keV at t_d. The observed low- and high-energy burst spectrum, $F\nu \propto \nu^{0.24}$ and $F\nu \propto \nu^{-1.22}$, respectively, require that $\nu_c \sim \nu_i \sim 50$ keV at t_d because, if ν_i or ν_c were below 50 keV, the spectrum below the peak of νF_ν would be $F_\nu \propto \nu^{-1/2}$ or steeper, while if ν_c were larger than ν_i the spectrum above the peak would be shallower than $F_\nu \propto \nu^{-1}$, assuming the electron index $p < 3$ implied by the decay of the optical afterglow.

Having ruled out all possibilities for producing γ-rays in a standard external shock (for $s = 0$), we now relax the assumption of time-independent ε_B in the FS. Since the peak synchrotron flux scales as $\varepsilon_B^{1/2} A_\nu^{(p-1)/2}$ and the synchrotron injection frequency as $\nu_i \propto \varepsilon_B^{1/2} A_\nu^{-1}$, an ε_B larger by a factor 100 at t_d and $A_\nu \sim 3$ simultaneously satisfy the observed γ-ray flux and the peak frequency requirements. The only remaining requirement to accommodate the burst properties with synchrotron emission from the forward shock is that $\nu_{cf}(t_d) \sim 50$ keV. We calculate the cooling frequency below to determine whether $\nu_{cf}(t_d) \sim 50$ keV is compatible with other constraints.

The Compton parameter in the forward shock at the deceleration time is obtained from equation (49). For $Y > 1$ and $p = 2.5$ this is given by

$$Y = 2\times 10^3 \varepsilon_{B_{f-4}}^{-1/3} \varepsilon_{\rm e}'^{5/3} (A_{\rm f} A_\nu)^{1/3} t_{\rm d}^{-1/6}. \quad (56)$$

Substituting this into equation (42) we find the cooling frequency in the forward shock for $z = 1$:

$$\nu_{\rm cf} = 7\times 10^9 \frac{\mathcal{E}_{52}^{1/2}}{\varepsilon_{B_{f-4}}^{5/6} \varepsilon_{\rm e}'^{22/3} A_\nu^{14/3} t_{\rm d}^{1/6}} \ {\rm Hz}. \quad (57)$$

When $\nu_{\rm cf} < \nu_{\rm i}$ and $Y \gg 1$, $Y \approx (\varepsilon_{\rm e}/\varepsilon_{B_{\rm f}})^{1/2}$, and

$$\nu_{\rm cf} = 2\times 10^{11} \frac{(1+z)\mathcal{E}_{52}^{1/2}}{\varepsilon_{B_{f-4}}^{1/2} \varepsilon_{\rm e} \varepsilon_{\rm e}'^4 A_\nu^{7/2} t_{\rm d}^{1/2}} \ {\rm Hz}. \quad (58)$$

For $Y \ll 1$ the cooling frequency in FS can be obtained by setting $Y = 0$ in equation (42).

Substituting $\nu_{\rm cf} \sim 50$ keV $= 1.2 \times 10^{19}$ Hz into equation (57) gives

$$\varepsilon_{\rm e}' A_\nu^{7/11} \varepsilon_{B_{f-4}}^{5/44}(t_{\rm d}) = 0.055 \mathcal{E}_{52}^{3/44} t_{\rm d}^{-1/44}. \quad (59)$$

Combining this with equation (17) – under the assumption that $\varepsilon_{\rm e}'$ is time independent – and making use of the requirement that $\varepsilon_{B_{\rm f}}(t_{\rm d})/\varepsilon_{B_{\rm f}}(t = 11\ {\rm min}) \sim 10^2$ discussed earlier, we find the following constraint on various parameters:

$$\varepsilon_{B_{\rm f}}^{6/11}(t_{\rm d}) \mathcal{E}_{52}^{14/11} = 4.3 A_\nu^{6/11} t_{\rm d}^{1/11}. \quad (60)$$

This relation can be satisfied if we consider, for instance, $\mathcal{E}_{52} = 20$, $\varepsilon_{B_{\rm f}}(t_{\rm d}) \sim 10^{-2}$ and $A_\nu \sim 1$. Thus we have a self-consistent solution that accounts for γ-ray and optical radiation for GRB 021211.

Fig. 2 shows the parameter space allowed by the γ-ray flux for 021211 originating in the forward shock. Note that there is a range of parameters for which the early and late optical and γ-ray observations can be explained simultaneously. The general requirements are: (i) a large magnetic field in the ejecta; (ii) a somewhat smaller field in the forward shock at deceleration; (iii) a much smaller $\varepsilon_{\rm Bf}$ at 11 min, when the forward shock emission starts to become a dominant contributor to the optical flux; and (iv) a low-density circumburst medium.

7.3 Radio flux limit at 10 d

The flux for GRB 021211 at 8.5 GHz, 10 d after the burst, is reported to be less than 35 μJy (Fox et al. 2003). The synchrotron peak frequency, which decays as $t^{-3/2}$, independent of circumburst medium stratification, is $10A_\nu^{-1}$ GHz at 10 d. If the radio band frequency were above the synchrotron self-absorption frequency, then the flux at 8.5 GHz should be 0.19 mJy independent of A_ν, which is a factor of 5.4 larger than the observed upper limit.

We consider the possibility that the self-absorption frequency is larger than 8.5 GHz, thereby reducing the flux below the observational upper limit. The FS self-absorption frequency, calculated using equations (13), (17)–(19), is

$$\nu_{\rm A}(\nu_{\rm i}/\nu_{\rm A})^{1/6} = 0.26 \frac{\varepsilon_{\rm Bf,-4}^{1/4} \Gamma_{\rm d,2}^2 n_0^{3/4} t_{\rm d}^{3/4}}{(1+z)^{3/2} \varepsilon_{\rm e}'^{1/2}} t^{-1/4}\ {\rm GHz}$$
$$= 24 A_\nu^{p/2} \mathcal{E}_{52}^{-1/2} \varepsilon_{\rm e}'^{1/2} t^{-1/4}\ {\rm GHz}. \quad (61)$$

Thus, $\nu_{\rm A} \sim 0.12$ GHz at 10 d for $A_\nu = 4$, $\mathcal{E}_{52} = 10$ and $\varepsilon_{\rm e}' = 0.03$. We see that A_ν should be ∼100 in order that $\nu_{\rm A} \sim 20$ GHz, so that the flux in the 8.5-GHz band at 10 d is below 35 μJy. However, for $A_\nu \sim 100$, equations (17) and (19) lead to $n \sim 2\times 10^6$ cm^{-3} and $\varepsilon_{\rm Bf}(t = 11\ {\rm min}) \sim 10^{-8}$, which are in contradiction with $n \sim 10^{-2}$ cm^{-3} and $\varepsilon_{\rm Bf}(t = 11\ {\rm min}) \sim 10^{-4}$ required to produce γ-ray emission in the external shock (see Fig. 2).

A reduction of fireball energy $\mathcal{E}$ by a factor of approximately 10 between 11 min and 10 d would also reduce the radio flux to a value below the observational upper limit, as the peak flux and synchrotron peak frequency are proportional to $\mathcal{E}$ and $\mathcal{E}^{1/2}$, respectively. This requirement is, however, inconsistent with the fact that most electrons are adiabatic ($\nu_{\rm c} > \nu_{\rm i}$) at all times, which results from $\nu_{\rm c}(t_{\rm d}) \sim \nu_{\rm i}(t_{\rm d})$ and that $\nu_{\rm i}$ decreases faster than $\nu_{\rm c}$.

The radio flux at 10 d can be reduced by a factor of ∼2 if the ejecta is collimated, such that they undergo lateral spreading before 10 d. From the isotropic equivalent of energy in 021211 of $\mathcal{E} = 2\times 10^{53}$ erg, estimated from early optical data (Section 7.1) and the typical jet energy of 10^{51} erg found by Frail et al. (2001), Piran et al. (2001) and Panaitescu & Kumar (2002), we obtain a jet opening angle of 8°. For $n \sim 10^{-2}$ cm^{-3} (see Fig. 2), the jet break time is expected at approximately 10 d, consistent with the lack of a clear break in the optical light curve.

A reduction by another factor of ∼2 in the radio flux could arise from a decreasing ε_B by a factor of 2 between 11 min and 10 d, as the flux above $\nu_{\rm i}$ scales as $\varepsilon_B^{(p+1)/4}$. We note that the observed $t^{-0.82}$ decline of the optical emission, together with the optical spectrum of $\nu^{-0.9}$, limit the decay of ε_B between 11 min and 10 d to be less than a factor of ∼3.

These above effects could then reconcile the late-time radio flux in the model considered here with the observational upper limit.

7.4 TeV flux limit during GRB

Milagro reported an upper limit of 4×10^{-6} erg cm^{-2} on the 0.2–20 TeV fluence for GRB 021211 (McEnery et al. 2002). Because $\nu_{\rm ir}(t_{\rm d}) < \nu_{\rm cr}(t_{\rm d})$, the peak of the inverse-Compton power from the reverse shock is at $\nu_{\rm c}\gamma_{\rm c}^2 \sim 100$ MeV, and the fluence in the Milagro band is $\sim 10^{-8}$ erg cm^{-2}. The IC emission in the forward shock peaks at $\nu_{\rm i}\gamma_{\rm i}^2 \sim 10$ TeV and the fluence in 0.2–20 TeV is $\sim Y\nu_{\rm if}F_{\rm p,f}t_{\rm d} \sim 5\times 10^{-7}$ erg cm^{-2}, i.e. smaller than the Milagro upper limit by an order of magnitude.

7.5 A summary of results for a uniform-density medium

A uniform-density medium cannot simultaneously explain the *R*-band afterglow emission after 11 min (FS emission) and before 11 min (presumably from the RS) for 021211 unless the energy density in the magnetic field in the RS is at least a few hundred times larger than the magnetic energy density in FS. Moreover, the γ-ray emission can be produced via the synchrotron process in the forward shock provided that the magnetic field parameter (ε_B) in FS at deceleration is larger by a factor of $\sim 10^2$ compared with the value at 11 min, i.e. we require a time-dependent $\varepsilon_{B_{\rm f}}$ during the first few minutes if γ-ray emission is to be produced in the external shock. The upper limit on radio flux at 10 d requires a combination of a jet break at approximately 10 d and a decline of ε_B by a factor of ∼2 between 11 min and 10 d.

8 PRE-EJECTED WIND CIRCUMBURST MEDIUM ($s = 2$)

8.1 Optical emission from a reverse shock

The synchrotron injection frequency and the flux at the peak of the RS spectrum are given by equations (29) and (32). For $p = 2.5$, $\mathcal{E}_{52} = 10$, $A_\nu = 4$, $A_{\rm f} = A_\nu^{(p-1)/2} = 2.8$, $t_{\rm d} = 2$ s, $\eta = 4$ and $\varepsilon_{\rm e}' = 0.05$, we find $\nu_{\rm ir} = 1.3\times 10^{13} \varepsilon_{\rm Br,-4}^{1/2}$ Hz and $F_{\rm p,r} = 7.4 \varepsilon_{\rm Br,-4}^{1/2}$ Jy; note that $\Gamma_{\rm d} = 230$, $A_* = 0.03$ and $\varepsilon_{\rm Bf}(t = 11\ {\rm min}) = 1.7\times 10^{-5}$ for this choice of parameters. The resulting R-band flux at 90 s is $\lesssim$0.5 mJy or a factor of 15 smaller than the observed value, if $\varepsilon_{\mathrm{Br},-4} = 1$. The model flux agrees with the observations for $\varepsilon_{\mathrm{Br}} \sim 10^{-2}$, provided that the absorption frequency is below the R band and the cooling frequency is sufficiently high ($\nu_{\mathrm{cr}} \sim 10^{17}$ Hz) so that the RS electrons continue to radiate in the R band until ∼11 min.

For the parameters considered above, the self-absorption frequency at deceleration (equation 34) is $\sim 10^{14}$ Hz, i.e. below the optical domain. The calculation of the cooling frequency proceeds in the same manner as for the $s = 0$ case considered in the previous section, and for $p = 2.5$ this is given by

$$\nu_{\mathrm{cr}} = 9.5 \times 10^{7} \frac{\mathcal{E}_{52}^{1/2} t_{\mathrm{d}}}{\varepsilon_{\mathrm{e}}^{\prime 7.7} \varepsilon_{B_{r-4}}^{0.83} \eta^{1.1} A_{\nu}^{5}} \ \mathrm{Hz}, \tag{62}$$

so long as $Y \gtrsim 1$. For $Y \ll 1$ the cooling frequency is given by setting $Y = 0$ in equation (42).

The requirement that $\nu_{\mathrm{cr}}(t_{\mathrm{d}}) > 10^{17}$ Hz leads to

$$\varepsilon_{\mathrm{e}}' \lesssim \frac{0.067 \mathcal{E}_{52}^{1/15.4} t_{\mathrm{d}}^{1/7.7}}{\varepsilon_{\mathrm{Br},-4}^{1/9} A_{\nu}^{2/3} \eta^{1/7}}, \tag{63}$$

from where it follows that

$$\nu_{\mathrm{ir}}(t_{\mathrm{d}}) \lesssim 1.5 \times 10^{12} \varepsilon_{\mathrm{Br},-4}^{1/6} \mathcal{E}_{52}^{1/5.1} A_{\nu}^{-1.1} \eta^{1.37} t_{\mathrm{d}}^{-0.6} \ \mathrm{Hz}, \tag{64}$$

$$F_{\mathrm{p,r}}(t_{\mathrm{d}}) \lesssim 660 \varepsilon_{\mathrm{Br},-4}^{1/3} \mathcal{E}_{52}^{0.85} A_{\nu}^{7/20} \eta^{-0.7} t_{\mathrm{d}}^{-0.55} \ \mathrm{mJy} \tag{65}$$

and the flux in the R band at the deceleration time is

$$F_{\nu_R}(t_{\mathrm{d}}) \lesssim 8.5 \varepsilon_{\mathrm{Br},-4}^{0.46} \mathcal{E}_{52} A_{\nu}^{-7/16} \eta^{0.3} t_{\mathrm{d}}^{-1.1} \ \mathrm{mJy}. \tag{66}$$

The flux in the R band at 90 s is therefore $2.6 \times 10^{-3} \varepsilon_{\mathrm{Br},-4}^{0.46} \mathcal{E}_{52} A_{\nu}^{-7/16} \eta^{0.3} t_{\mathrm{d}}^{0.7}$ mJy. This is smaller than the observed value of 7.2 mJy even for $\varepsilon_{\mathrm{Br}} = 1$, $\mathcal{E}_{52} = 20$ and $A_{\nu} = 1$. Thus, to obtain the observed optical flux at 90 s in a pre-ejected wind model, requires very extreme and, perhaps, unphysical parameters. More accurate numerical calculations support this conclusion.

8.2 γ-ray emission

The arguments given for $s = 0$ against synchrotron self-Compton in reverse or forward shock as an explanation for the γ-ray properties, also apply to $s = 2$. Once again synchrotron radiation from the forward shock remains the most likely mechanism for GRB 021211.

For a time-independent ε_B in the forward shock, the synchrotron injection frequency at $t_{\mathrm{d}} = 2$ s, $13 A_{\nu}^{-1}$ keV, is a factor of ∼4 smaller than the observed peak frequency of νF_{ν}. The peak flux $3.6 A_{\mathrm{f}}$ mJy is comparable with that observed. A slightly larger $\varepsilon_{\mathrm{Bf}}$ at deceleration than at 11 min can yield the right value for $\nu_{\mathrm{i}}(t_{\mathrm{d}})$. As discussed in the previous section, the spectrum of GRB 021211 requires that $\nu_{\mathrm{cf}} \sim 50$ keV. We compute the cooling frequency below to determine whether this condition can be satisfied for $s = 2$.

For $p = 2.5$ and $Y > 1$ the Compton parameter is obtained from equation (49) and is given by

$$Y \approx 8.7 \times 10^{3} \varepsilon_{B_{f-4}}^{-1/3} \varepsilon_{\mathrm{e}}^{\prime 5/3} A_{\nu}^{7/12} t_{\mathrm{d}}^{-1/3}. \tag{67}$$

Substituting this into equation (42) we find the cooling frequency in the forward shock at the deceleration time:

$$\nu_{\mathrm{cf}} = 1.5 \times 10^{7} \frac{\mathcal{E}_{52}^{1/2} t_{\mathrm{d}}^{7/6}}{\varepsilon_{B_{f-4}}^{5/6} \varepsilon_{\mathrm{e}}^{\prime 22/3} A_{\nu}^{14/3}} \ \mathrm{Hz}. \tag{68}$$

For $Y \ll 1$ the cooling frequency is obtained by setting $Y = 0$ in equation (42).

Since the peak of the γ-ray spectrum for 021211 is at $\nu_{\mathrm{cf}} \sim \nu_{\mathrm{if}} = 1.2 \times 10^{19}$ Hz, we obtain from equation (68) the following relation:

$$\varepsilon_{\mathrm{e}}' A_{\nu}^{7/11} \varepsilon_{B_{\mathrm{f}}}^{5/44}(t_{\mathrm{d}}) = 8.4 \times 10^{-3} \mathcal{E}_{52}^{3/44} t_{\mathrm{d}}^{7/44}. \tag{69}$$

Using equations (23) and (69), and taking $\varepsilon_{B_{\mathrm{f}}}(t_{\mathrm{d}})/\varepsilon_{B_{\mathrm{f}}}(t = 11\ \mathrm{min}) \sim 10$ as discussed at the beginning of this subsection, we find

$$\varepsilon_{B_{\mathrm{f}}}^{6/11}(t_{\mathrm{d}}) \mathcal{E}_{52}^{14/11} t_{\mathrm{d}}^{7/11} = 33 A_{\nu}^{6/11}. \tag{70}$$

This equation can be satisfied if we take $\mathcal{E}_{52} = 30$, $\varepsilon_{B_{\mathrm{f}}}(t_{\mathrm{d}}) \sim 0.1$, $t_{\mathrm{d}} \sim 2$s and $A_{\nu} \sim 1$. Note that for these parameters the density of the medium $A_{*} \sim 5 \times 10^{-4}$, which is three orders of magnitude smaller than the value for a typical Wolf–Rayet star wind. Thus we find that the $s = 2$ model has difficulty in accommodating the early optical and γ-ray flux for 021211.

8.3 Radio flux upper limits

The FS peak flux declines as $5 A_{\mathrm{f}} t^{-1/2}$ mJy, therefore the peak flux at 10 d is ∼6 μJy. The expected flux at 8.5 GHz, 10 d after the explosion, is thus less than 5.8 μJy, entirely consistent with the upper limit of ∼35 μJy.

The peak frequency for the RS emission declines as $t^{-17/12}$ and the peak flux declines as $\sim t^{-1}$. Therefore, the peak frequency and flux at 0.1 d are 0.8 GHz and 1.0 mJy, respectively. The absorption frequency decreases as $\nu_{\mathrm{A}} \propto t^{-5/6}$ and thus $\nu_{\mathrm{A}} \sim 110$ GHz at 0.1 d. Therefore, the flux at 8.5 GHz at 0.1 d is expected to be approximately 6 μJy, which is well below the upper limit reported by Fox et al. (2003).

9 DISCUSSION

It is widely believed that γ-ray emission for highly variable GRBs is produced in internal shocks (Rees & Mészáros 1994). However, the γ-ray light curve for a burst consisting of a single peak (fast rise and exponential decay), such as GRB 021211, could arise in an external shock. In this paper, we have attributed the gamma-ray and the afterglow emissions of GRB 021211 to the reverse and forward shocks occurring in the interaction between a relativistic fireball and the circumburst medium.

The burst and early afterglow measurements of GRB 021211 constrains the various afterglow parameters, as follows. The optical flux from the reverse shock measured at 90 s, requires a magnetic field parameter $\varepsilon_{\mathrm{Br}} \sim 0.1$ behind the RS at the deceleration time-scale, and a fireball kinetic energy (isotropic equivalent) of $\mathcal{E} \sim 10^{53}$ erg. The condition that the cooling frequency for the RS does not fall below the optical domain until 11 min sets an upper limit $\varepsilon_{\mathrm{e}}' < 0.1$ on the parameter for the minimal electron energy behind the RS. The synchrotron radiation from the RS can also explain the observed γ-ray fluence and the peak frequency of the GRB spectrum for a suitable choice of parameters, however, it cannot account for the hard low-energy spectral slope observed in GRB 021211. Therefore, for the external shock model considered in this paper the GRB emission can only be synchrotron radiation from the forward shock. The observed peak flux requires that the magnetic field behind the FS is $\varepsilon_{\mathrm{Bf}} \sim 10^{-2}$ at deceleration. Furthermore, the burst spectrum indicates that the injection and cooling frequencies at deceleration are both around 50 keV, which requires that $\varepsilon_{\mathrm{e}}' \sim 0.01$ for the FS and that the peak of the synchrotron emission at 11 min is only slightly below the optical domain. The latter leads to that $\varepsilon_{\mathrm{Bf}} \sim 10^{-4}$ at 11 min, which, together with the observed FS flux at 11 min, requires that the external density is $n \lesssim 10^{-2}$. Finally, the observed burst duration determines the deceleration time-scale which, for the above density, leads to an initial Lorentz factor of the fireball of $\Gamma \sim 1500$.

Therefore, we find that, at deceleration, the magnetic field parameter ε_B in the RS and FS is three and two orders of magnitude larger, respectively, than behind the FS at 11 min. Zhang, Kobayashi & Mészáros (2003) have suggested that the bright optical flash of GRB 990123 also requires a high magnetic field in reverse shock, however, they find $\varepsilon_{\rm Br} \sim \varepsilon_{\rm Bf}$ for 021211. This combination of a high ε_B in the ejecta and high, but somewhat smaller, ε_B in the FS at the deceleration suggests that the magnetic field in the RS is the leftover, frozen-in field of an initially highly magnetized outflow as suggested by Usov (1992), Mészáros & Rees (1997), Lyutikov & Blandford (2002), and that the field in the early FS results from the mixing of the ejecta with the shocked circumburst medium.

The transverse magnetic field in the ejecta decays as R^{-1} at early times, when the radial width of the material ejected in the explosion (δR) is constant, and the total energy in the magnetic field is conserved. Therefore, if an explosion puts out equal amounts of energy in the magnetic field and the relativistic ejecta, the equipartition will continue to hold until δR starts to increase. For a burst of duration T and Lorentz factor Γ, $\delta R \sim \max\{cT, R/\Gamma^2\}$, and so δR increases only when $R \gtrsim cT\Gamma^2$. At large R, the magnetic field decays as R^{-2} and the energy in the magnetic field decreases as $1/R$. For GRB 021211, $T \sim 4$s and $\Gamma \sim 10^3$, thus we expect a substantial fraction of the explosion energy to be in the magnetic field at the deceleration radius of $\sim 10^{17}$ cm, if the burst was initially Poynting-flux-dominated.

A uniform, but very tenuous medium in the vicinity of the burst is consistent with the burst properties and early- and late-time optical data, but an r^{-2} density profile is disfavoured, as it requires at 10^{17} cm a density smaller by a factor $\gtrsim 10^4$ than that expected for a Wolf–Rayet star. The upper limit on radio flux at 8.5 GHz at 10 d (Fox et al. 2003) poses a problem for the uniform density medium. The solution requires a combination of jet break at approximately 10 d and a decrease in ε_B by a factor of ~ 2 between 11 min and 10 d.

A time-dependent energy in the fireball could explain the GRB emission and the early afterglow observations simultaneously provided that the fireball energy during the burst is a factor ~ 10 larger compared with the energy at 11 min. However, the radiative loss of energy for 021211 is quite small – as $\epsilon_e < 0.1$ in order to satisfy the requirement, imposed by the observed low-energy slope of the γ-ray spectrum, that the cooling frequency in the forward shock at deceleration be 50 keV – thereby ruling out this possibility.

An upper limit on the number of electrons and positrons per proton in the ejecta is set by the fact that the reverse shock synchrotron radiation becomes softer with increasing numbers of leptons. When this number exceeds 10, the reverse shock emission yields at 0.1 d an 8.5-GHz flux that exceeds the observational upper limit by more than an order of magnitude.

ACKNOWLEDGMENTS

We thank Erin McMahon, Ramesh Narayan and Brad Schaefer for useful discussions

REFERENCES

Crew G. et al. 2003, ApJ, submitted (astro-ph/0303470)
Fox D. et al., 2003, ApJ, 586, L5
Frail D. et al., 2001, ApJ, 562, L55
Fruchter A., Andrew L., Vreeswijk P., Holland S. T., Kouveliotov K., 2002, GCN 1781
Greiner J. et al., 2003, GCN 2020
Kobayashi S., 2000, ApJ, 545, 807
Li W., Filippenko A., Chornock R., Jha S., 2003, ApJ, 586, L9
Lyutikov M., Blandford R.D., 2002, in Ouyed R., Hjorth J., Nordlund A., eds, Beaming and Jets in Gamma-ray Bursts, preprint astro-ph/0210671
McEnery J. et al., 2002, GCN 1740
Matheson T. et al., 2003, GCN 2120
Mészáros P., Rees M., 1993, ApJ, 405, 278
Mészáros P., Rees M., 1997, ApJ, 482, 29
Panaitescu A., Kumar P., 2002, ApJ, 571, 779
Panaitescu A., Mészáros P., 1998, ApJ, 492, 683
Panaitescu A., Mészáros P., 2000, ApJ, 544, L17
Piran T., 1999, Phys. Rep., 314, 575
Piran T., Kumar P., Panaitescu A., Piro L., 2001, ApJ, 560, L167
Rees M.J., Mészáros P., 1994, ApJ, 430, L93
Sari R., Piran T., 1999, ApJ, 517, L109
Usov V., 1992, Nat, 357, 472
Wijers R., Rees M., Mészáros P., 1997, MNRAS, 288, L51
Wozniak P. et al., 2002, GCN 1757
Zhang B., Kobayashi S., Mészáros P., 2003, ApJ, 595, 950

This paper has been typeset from a TEX/LATEX file prepared by the author.